©2016 Published in 4th International Symposium on Innovative Technologies in Engineering and Science 3-5 November 2016 (ISITES2016 Alanya/Antalya - Turkey)

Experimental Performance Analysis of an R134a Automobile Air Conditioning and Air-Sourced Heat Pump System

*Murat HOŞÖZ, Erkutay TAŞDEMİRCİ and Ertan ALPTEKİN
Faculty of Technology, Department of Automotive Engineering, Kocaeli University, Turkey

Abstract

Experimental performance of an R134a automobile air conditioning (AAC) system capable of operating as an air-sourced automotive heat pump (AHP) has been evaluated in cooling and heat pump operations. For this aim, an experimental system was made up from the original components of an AAC system. The system was tested at five different compressor speeds. For cooling mode operations, the temperatures of the air streams entering the evaporator and condenser were maintained at $T_{evap,ai}$=25°C – $T_{cond,ai}$=25°C and $T_{evap,ai}$=30°C –$T_{cond,ai}$=30°C. On the other hand, for heat pump operations, the inlet temperatures were maintained at $T_{evap,ai}$=0°C – $T_{cond,ai}$=0°C and $T_{evap,ai}$=10°C – $T_{cond,ai}$=10°C. Using experimental data, performance parameters such as conditioned air stream temperature, compressor power, compressor mechanical power and compressor discharge temperature were evaluated in both operation modes. Furthermore, the cooling capacity and coefficient of performance for cooling (COP_c) were evaluated in cooling mode, while the heating capacity and coefficient of performance for heating (COP_h) were evaluated in heat pump mode. The cooling capacity and compressor power increased but COP_c decreased with rising compressor speed. The system operating in heat pump mode provided sufficiently high heating capacity and conditioned air stream temperatures. Furthermore, the heating capacity increased but COP_h decreased with rising compressor speed.

Key words: R134a, automobile, air conditioning, heat pump

1. Introduction

Comfort heating of the passenger compartment of motor vehicles is commonly achieved utilizing waste heat recovered from the engine coolant. However, in some extreme conditions the available waste heat is not enough to achieve a comfortable compartment temperature. The lack of sufficient waste heat is more critical for vehicles employing diesel engines. It is known that some high efficiency-direct injection diesel engines cannot produce sufficient waste heat to achieve thermal comfort in a short time period [1]. In order to provide sufficiently high compartment temperatures after starting up the engine, some vehicles utilize supplemental heaters relying on fuel or electricity in expense of high initial and operating costs, low efficiency, air pollution and global warming.

Use of hybrid and electric vehicles are rapidly increasing due to the concerns about environmental issues such as global warming. However, these types of vehicles have little or no waste heat. Therefore, required comfort heating is provided by using electric energy, which in turn causes an increase in the specific energy consumption. One of the appropriate solutions for this problem is to operate the present air conditioning system as a heat pump by using the

*Corresponding author: Address: Faculty of Technology, Department of Automotive Engineering, Kocaeli University, 41380, Kocaeli TURKEY. E-mail address: mhosoz@kocaeli.edu.tr, Phone: +902623032279

environmental air as a heat source. For this aim, certain low cost components can be added to the present air conditioning system of the vehicle to perform heat pump operation [2]. The automotive heat pump (AHP) system developed in this way can be used providing comfort heating to the passenger compartment individually or it can provide supplemental heating to the passenger compartment.

There are only a few research studies on the AHP systems in the literature because of competition in this area. Vargas and Parise [3] established a mathematical model for the performance of a heat pump system with a variable capacity compressor. Antonijevic and Heckt [4] evaluated the performance of an R134a AHP system used for providing supplemental heating to the passenger compartment. They determined that the ratio of the heating capacity to the fuel consumption of the developed system was significantly better compared to other alternative supplemental heating systems. Domitrovic et al. [5] simulated the steady-state cooling and heating operation of an automotive air conditioning (AAC) and AHP system. Hosoz and Direk [6] evaluated the performance of an air-to-air R134a AHP system. Rongstam and Mingrino [7] evaluated the performance of an R134a AHP system using engine coolant as a heat source in comparison to the performance of the coolant-based heating system. Lee et al. [8] investigated the performance characteristics of a mobile heat pump for an electric bus employing the wasted heat of electric devices as a heat source. Scherer et al. [9] compared the performance of R152a and R134a in an AHP system using engine coolant as a heat source. Direk and Hosoz [10] performed energy and exergy analyses of an R134a AHP system using ambient air as a heat source. Tamura et al. [11] investigated the experimental performance of an AHP system using CO_2 as a refrigerant. Kim et al. [12] also studied the heating performance of an AHP system using CO_2.

In this study, the performance parameters of an experimental AAC system with the capability of operating as an AHP system using ambient air as a heat source were evaluated for the cases of cooling and heat pump mode operations.

2. Description of the Experimental Setup

The experimental AAC/AHP system was generally made up from the original components of an AAC system belonging to a D segment car, as shown schematically in Figure 1. It employed a seven-cylinder fixed-capacity swash-plate compressor, a parallel-flow micro-channel outdoor coil, a laminated type indoor coil, two thermostatic expansion valves (TXVs), a reversing valve to operate the system in reverse direction in the heat pump mode and some auxiliary components. Figure 2 shows a photograph of the experimental AAC/AHP system, and Table 1 indicates the specifications of the components used in the system.

The indoor and outdoor units were inserted into separate air ducts, each with a length of 1.0 m. The indoor and outdoor ducts were equipped with a centrifugal fan and an axial fan, respectively. These ducts were also equipped with electric heaters located upstream of the indoor and outdoor units. The indoor and outdoor duct electric heaters could be controlled between 0–2.5 kW and 0–4.5 kW, respectively, to provide the required air temperatures at the inlets of the indoor and outdoor units. The refrigeration circuit was charged with 3200 g of R134a.

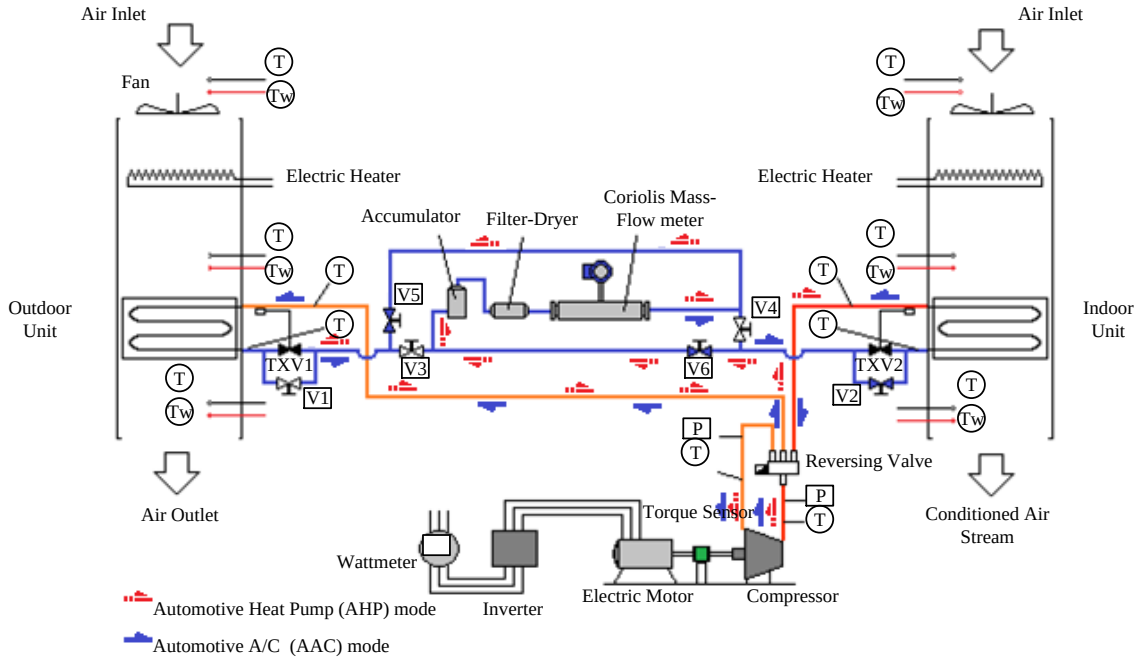

Figure 1. Schematic illustration of the experimental AAC/AHP system.

Figure 2. Photograph of the experimental AAC/AHP system.

In order to acquire data for performance evaluation, some mechanical and electrical measurements were performed on the system. The employed instruments and their locations are also indicated in Figure 1. The refrigerant mass flow rate was measured by a Coriolis mass flow meter. The temperature measurements were performed by type K thermocouples, and refrigerant pressures were measured by both pressure transmitters and Bourdon gauges. Most of the measured variables were acquired through a data acquisition system, and recorded on a computer. The characteristics of the instrumentation can be seen in Table 2.

Table 1. Specifications of the components of the AAC/AHP system.

Components	Specifications
Compressor	Type: fixed-capacity swash-plate, stroke volume: 155 cc, no. of cylinders: 7, max. speed: 6000 rpm
Indoor unit	Type: laminated coil, capacity: 5.8 kW, dimensions: 260 × 230 × 100 mm^3, no. of channels: 23
Outdoor unit	Type: parallel-flow micro-channel coil, capacity: 7.5 kW, dimensions: 600 × 400 × 17 mm^3, no. of channels: 42
TXVs	Type: internally equalized with bulb
Electromagnetic Clutch	48 W (12 V) electromagnetic type
Indoor unit fan	100 W (12 V) centrifugal type
Outdoor unit fan	2 x 75W (12 V) 300 mm diameter axial flow fan

Table 2. Characteristics of the instrumentation.

Measured variable	Instrument	Range	Accuracy
Temperature	Type K thermocouple	−50 to 500 °C	±0.5 °C
Pressure	Pressure transmitter	0 to 25 bar	±0.2 % full scale
Humidity	Hygrometer	10 to 100%	± 3% full scale
Air flow rate	Anemometer	0.1 to 15 m s^{-1}	± 3 %full scale
Refrigerant mass flow rate	Coriolis flow meter	0 to 1,300 kg h^{-1}	± 0.1% full scale
Compressor speed	Digital tachometer	10 to 100,000 rpm	± 0.1 % reading +2 rpm
Torque	Non-contact shaft to shaft torque sensor	-50 to 50 Nm	±0.05%full scale

The AHP system was driven by an electric motor with a maximum power of 5.50 kW at 2925 rpm. The motor torque was measured by a torque sensor placed on the shaft between the electric motor and compressor.

Figure 1 also illustrates the refrigerant flow paths in the experimental AAC/AHP for both operation modes. In order to perform the heat pump (HP) operation, the reversing valve is energized. Then, the reversing valve directs the high temperature superheated vapour refrigerant discharged from the compressor to the indoor unit (condenser). The refrigerant passing through the indoor unit rejects heat into the indoor air stream, thus providing a warm air stream to the passenger compartment. As a result, the refrigerant condenses and leaves the indoor unit as subcooled liquid. In HP operation, the thermostatic expansion valve 2 (TXV2) is bypassed. Then, the refrigerant flows through the valves V2 and V6, and reaches the receiver tank, which keeps the unrequired refrigerant in it when the thermostatic expansion valve decreases the refrigerant flow rate at low loads. After passing through the filter/drier, sight glass, Coriolis flow meter and V5, the refrigerant reaches TXV1 located at the inlet of the outdoor unit. Since the valves V3 and V4 are closed, the refrigerant passes through TXV1, which reduces the pressure, and thereby the temperature of the liquid refrigerant. TXV1 also controls the refrigerant mass flow rate circulating through the circuit by keeping a constant superheat at the outlet of the outdoor unit. Then, the refrigerant enters the outdoor unit, in which it absorbs heat from the outdoor air stream,

and leaves this unit as low pressure superheated vapour. Then, the refrigerant enters the compressor via the reversing valve. The refrigerant leaves the compressor as a high pressure superheated vapour, and the cycle starts over.

In order to operate the system in air conditioning (cooling) mode, the reversing valve is deenergised. Then, the refrigerant discharged from the compressor is sent to the outdoor unit, where it condenses by rejecting heat into the outdoor air stream. Afterwards, the subcooled refrigerant passes through V1, filter/drier, sight glass, Coriolis flow meter, V3 and reaches the TXV2, which reduces the pressure as well as temperature. After absorbing heat from the air-conditioned air stream, the refrigerant is drawn into the compressor via the reversing valve, and the cycle starts over.

3. Thermodynamic Analysis

The performance parameters of the experimental AAC/AHP system can be evaluated by applying the first law of thermodynamics to the system. Using this law for the indoor unit (condenser) of the AHP system, the heating capacity of the AHP system can be evaluated from

$$\dot{Q}_{cond} = \dot{m}_r(h_{cond,in} - h_{cond,out}) \quad (1)$$

where $\dot{m}_r$ is the refrigerant mass flow rate. On the other hand, by applying the first law of thermodynamics to the indoor unit (evaporator) of the AAC system, the cooling capacity of the AAC system can be obtained from

$$\dot{Q}_{evap} = \dot{m}_r(h_{evap,out} - h_{evap,in}) \quad (2)$$

Assuming that the compressor is adiabatic, the power absorbed by the refrigerant during the compression process in both operation modes can be determined from

$$\dot{W}_{comp} = \dot{m}_r(h_{comp,out} - h_{comp,in}) \quad (3)$$

The shaft power input to compressor can be evaluated from the motor torque and speed, i.e.

$$\dot{W}_{comp,shaft} = T\frac{\pi n}{30} \quad (4)$$

The coefficient of performance of the AHP system is defined as the ratio between heating capacity and power input to the system, i.e.

$$COP_h = \frac{\dot{Q}_{cond}}{\dot{W}_{in}} \quad (5)$$

where $\dot{W}_{in}$ is the sum of compressor power and power inputs to the indoor unit blower, outdoor unit fan and compressor electromagnetic clutch.

The coefficient of performance of the AAC system, on the other hand, is defined as the ratio between cooling capacity and power input to the system, i.e.

$$COP_c = \frac{\dot{Q}_{evap}}{\dot{W}_{in}} \quad (6)$$

The coefficient of performance of the AHP system based on compressor shaft power input as well as other power inputs to the system can be obtained from

$$COP_{h,m} = \frac{\dot{Q}_{cond}}{\dot{W}_{in,m}} \quad (7)$$

where $\dot{W}_{in,m}$ is the mechanical power input to the AAC/AHP system, which is evaluated by summing up the shaft power input to the compressor and the power consumed by the fans of indoor and outdoor units as well as compressor electromagnetic clutch.

Finally, the coefficient of performance of the AAC system based on compressor shaft power input as well as other power inputs to the system can be obtained from

$$COP_{c,m} = \frac{\dot{Q}_{evap}}{\dot{W}_{in,m}} \quad (8)$$

4. Testing Procedure

Performance tests were carried out at six different compressor speeds, namely 800, 1200, 1600, 2000, 2400 and 2800 rpm. In all tests, the indoor and outdoor air flow rates were kept constant at 0.158 m^3/s and 0.728 m^3/s, respectively. Before performing the AHP tests, the air temperatures at the inlets of the evaporator ($T_{evap,\ ain}$) and condenser ($T_{cond,\ ain}$) were simultaneously fixed to 5 or 10 °C. Although data were collected continuously during the tests, only steady-state data were used in the performance evaluations. The steady-state was achieved in 10–15 min after starting up a test operation. During the AHP tests, discharge pressure was never allowed to exceed 16 bar, which was the maximum test pressure of the indoor coil. Using data acquired in the test operations, the air temperature at the outlet of the indoor coil, heating capacity, COP_h and $COP_{h,m}$ of the AHP system were evaluated. The enthalpies of the refrigerant were obtained from REFPROP [13] as a function of temperature and pressure data. After performing heat pump tests in winter months, the air conditioning (cooling) tests were conducted in summer months. Before performing the AAC tests, the air temperatures at inlets of the evaporator ($T_{evap,\ ain}$) and condenser ($T_{cond,\ ain}$) were simultaneously fixed to 25 or 30 °C. The procedures used in heat pump tests were the same as those used in air conditioning tests.

5. Uncertainty analysis

The uncertainty for each calculated performance parameter of the experimental system was determined using the method suggested by Moffat [14]. This method assumes that the function R is to be calculated from a set of totally N independent variables, i.e.

$$R = R(X_1, X_2, \dots, X_N) \quad (9)$$

The uncertainty of the result R can be determined by combining the uncertainties of the individual variables using a root-sum-square method as in the following.

$$\Delta R = \left[\sum_{i=1}^{N} \left(\frac{\partial R}{\partial X_i}\Delta X_i\right)^2\right]^{1/2} \quad (10)$$

Using the accuracies for the measured variables reported in Table 2 and evaluating Eqs. (1)–(8) in Eq.(10), the uncertainties of $\dot{Q}_{cond}$, $\dot{Q}_{evap}$, $\dot{W}_{comp}$, $\dot{W}_{comp,shaft}$, COP_h, COP_c, $COP_{h,m}$ and $COP_{c,m}$ were estimated as 2.8%, 2.6%, 3.0%, 0.05%, 4.1%, 4.0%, 2.8% and 2.6%, respectively.

6. Results and Discussion

6.1. Air Conditioning Mode

Various performance parameters of the experimental system for AAC tests are shown in Figures 3–6. The conditioned air temperature at the outlet of the indoor unit and compressor discharge temperature were shown in Figure 3 (a) and (b), respectively. The conditioned air temperature decreases slightly with compressor speed, and the lower the set of air inlet temperatures, the lower the conditioned air temperature. On the other hand, the compressor discharge temperature goes up with increasing compressor speed, and the higher the set of air inlet temperatures, the higher the compressor discharge temperature.

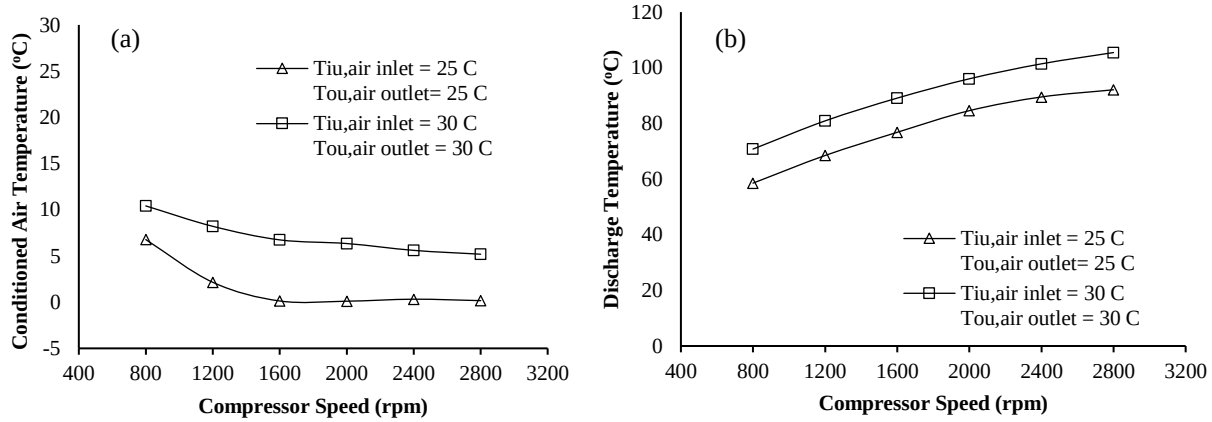

Figure 3. Variations in the conditioned air temperature (a) and discharge temperature (b) with compressor speed.

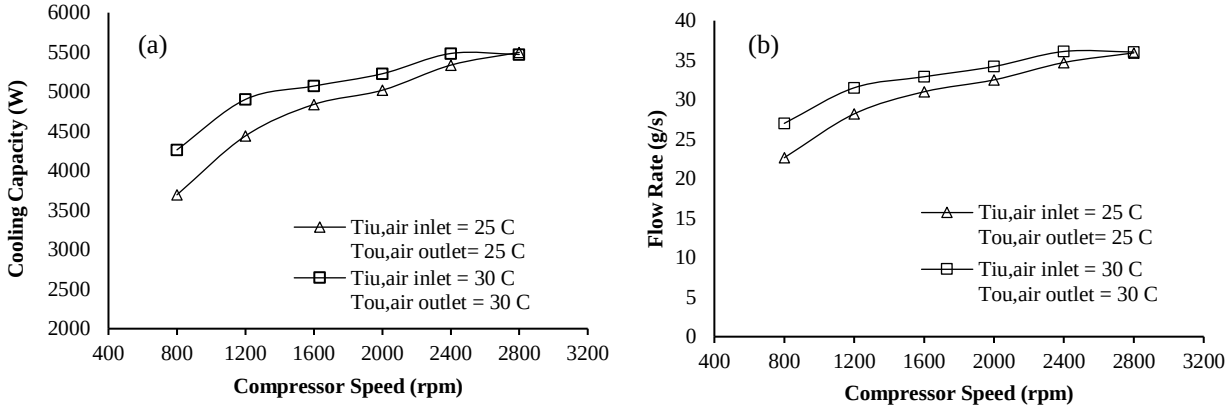

Figure 4. Variations in the cooling capacity (a) and refrigerant flow rate (b) with compressor speed.

The cooling capacity and refrigerant mass flow rate were shown in Figure 4 (a) and (b), respectively. The cooling capacity and refrigerant mass flow rate increases with rising compressor speed. The refrigerant mass flow rate rises with increasing air inlet temperature set.

The compressor power and compressor shaft power were shown in Figure 5 (a) and (b), respectively. It is seen that both compressor powers get higher considerably with increasing compressor speed, and the higher the inlet air temperature set, the higher the compressor power and compressor shaft power.

The coefficient of performance for cooling and the coefficient of performance based on compressor shaft power input were shown in Figure 6 (a) and (b), respectively. Because compressor power increase faster than cooling capacity does with rising compressor speed, both the COP_c and $COP_{c,m}$ decrease with it. It is seen that the higher the air inlet temperature set, the lower the COP_c and $COP_{c,m}$.

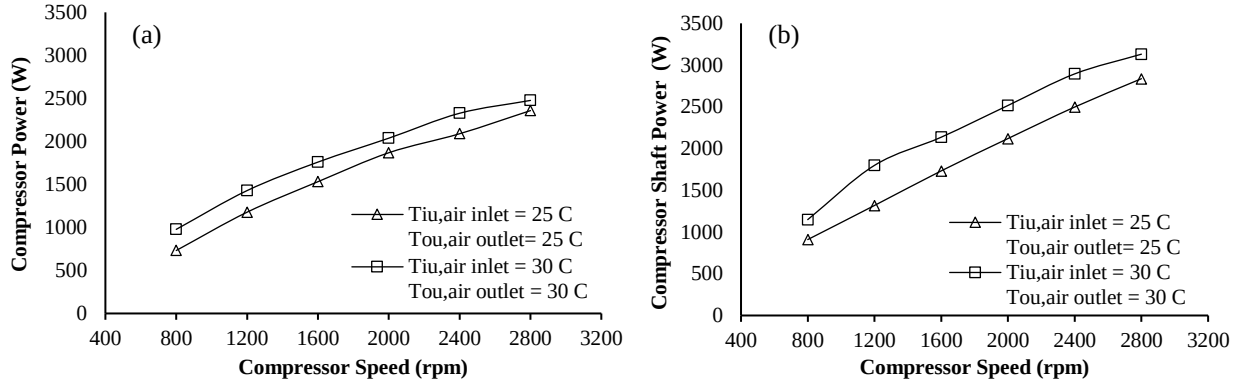

Figure 5. Variations in the compressor power (a) and compressor shaft power (b) with compressor speed.

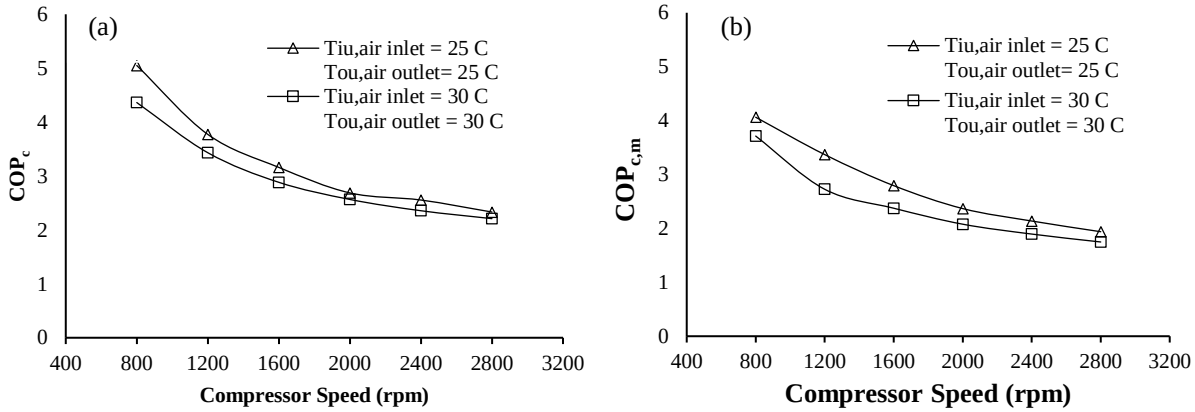

Figure 6. Variations in the coefficient of performance for cooling (a) and coefficient of performance based on compressor shaft power input (b) with compressor speed.

6.2. Heat Pump Mode

Various performance parameters of the experimental system for AHP tests are shown in Figures 7–10. The conditioned air temperature at the outlet of the indoor unit and compressor discharge temperature were shown in Figure 7 (a) and (b), respectively. The conditioned air temperature increases with compressor speed, and the higher the set of air inlet temperatures, the higher the conditioned air temperature. The compressor discharge temperature rises with increasing compressor speed, and it increases with rising air inlet temperature set.

The heating capacity and refrigerant mass flow rate were shown in Figure 8 (a) and (b), respectively. The heating capacity increases considerably with the compressor speed, while the refrigerant mass flow increases slightly with it. It is seen that the heating capacity and refrigerant mass flow rate rise with increasing air inlet temperature set.

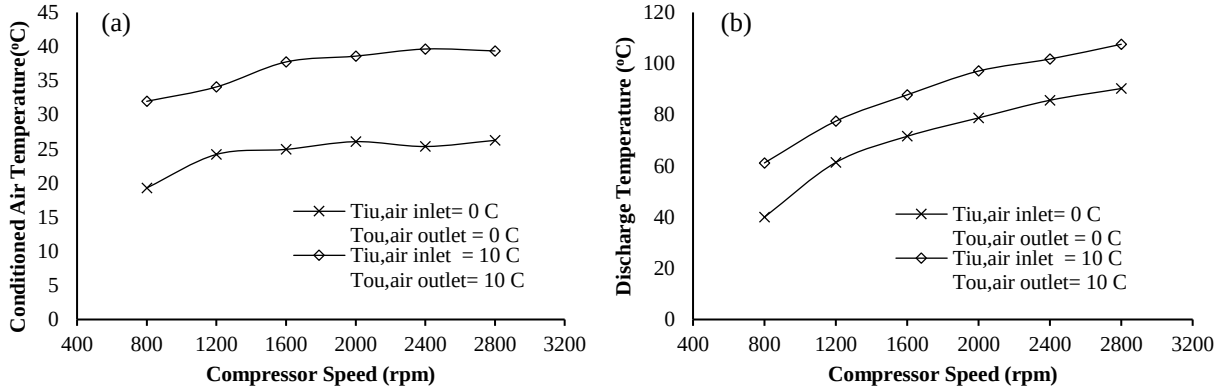

Figure 7. Variations in the conditioned air temperature (a) and discharge temperature (b) with compressor speed.

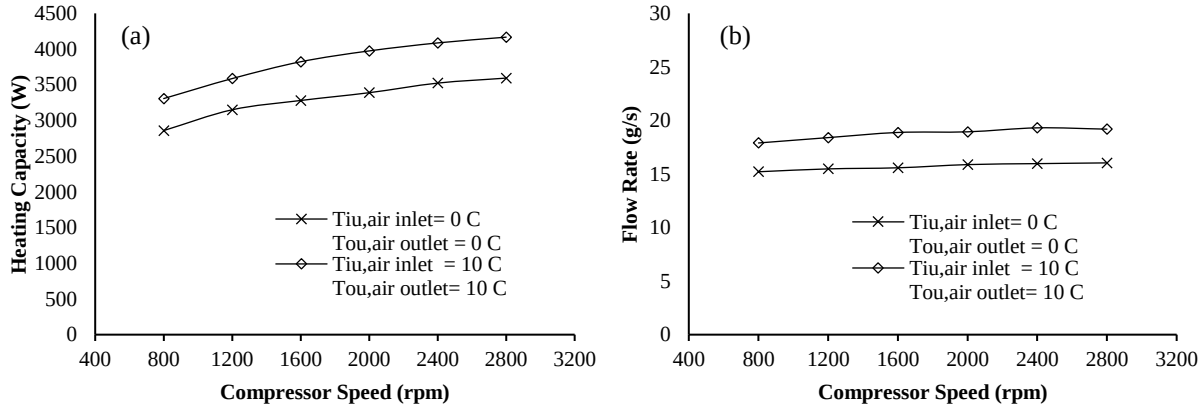

Figure 8. Variations in the heating capacity (a) and refrigerant flow rate (b) with compressor speed.

The compressor power and compressor shaft power were shown in Figure 9 (a) and (b), respectively. It is seen that both compressor powers get higher with increasing compressor speed and rising inlet air temperature set.

The coefficient of performance for heating and the coefficient of performance based on

compressor shaft power input were shown in Figure 10 (a) and (b), respectively. Both heating capacity and compressor power increase with rising compressor speed. However, because compressor power increases faster than the heating capacity does, both the COP_h and $COP_{h,m}$ decrease with it. The lower the air inlet temperature set, the higher the COP_h and $COP_{h,m}$.

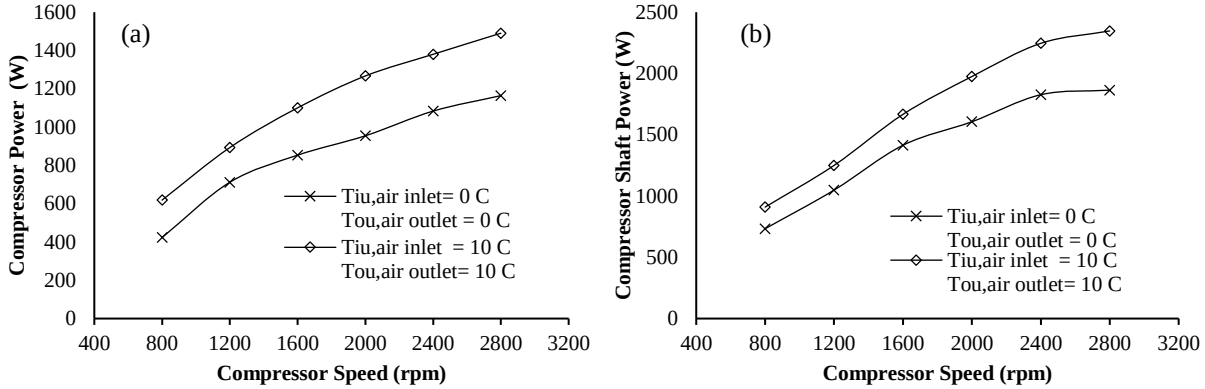

Figure 9. Variations in the compressor power (a) and compressor shaft power (b) with compressor speed.

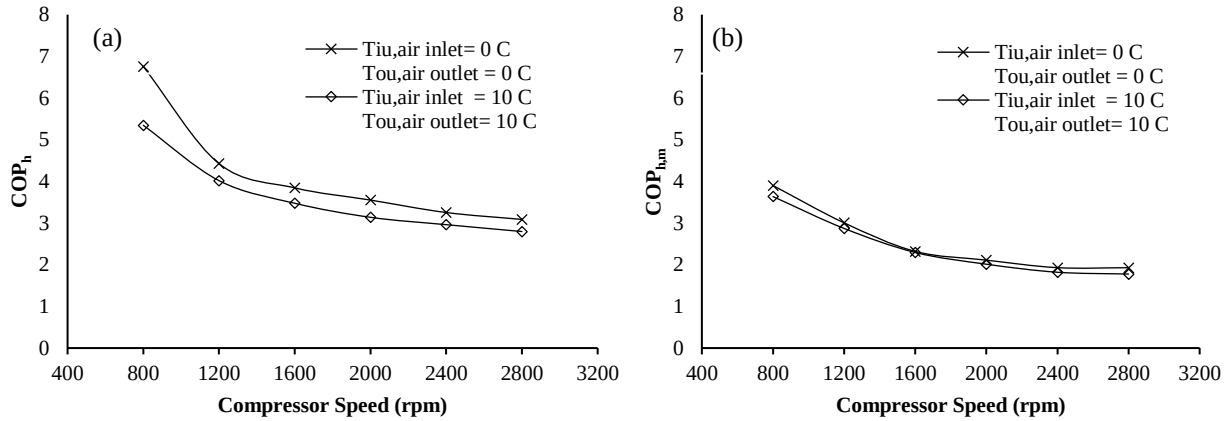

Figure 10. Variations in COP_h (a) and $COP_{h,m}$ (b) with compressor speed.

7. Conclusions

Various performance parameters of an automotive AAC/AHP system using R134a as the working fluid have been experimentally evaluated in both air conditioning and heat pump operations. The final conclusions reached in this study are as follows.

- The conditioned air temperature at the outlet of indoor unit decrease with compressor speed in AAC mode, while it increases with compressor speed in AHP mode. Although the conditioned air temperatures for 5°C air inlet temperature set are not sufficiently high, the AHP system provided high enough air temperatures for 10°C air inlet temperature set. Because the air-sourced AHP system cannot provide sufficient heating capacity at severe winter conditions, it can be used as a supplemental heating system.

- Both cooling and heating capacities of the system increase with compressor speed. However, both *COP* of the system for cooling and heating modes drop with rising compressor speed.
- Although the AHP provides insufficient heating capacity, it provides heating with *COP* values of as high as 6, which is 1 for electric heating. This means that AHP systems can perform heating with a high energetic performance compared to its alternatives.

Acknowledgements

The authors would like to acknowledge the support provided by Kocaeli University under the project number 2014/51.

References

[1] Wienbolt HW, Augenstein CD. Visco heater for low consumption vehicles. SAE Word Congress 2003;Detroit, Michigan, USA, Paper Code 2003-01-0738.
[2] Meyer J, Yang G, Papoulis E. R134a heat pump for improved passenger comfort, SAE Technical Papers 2004;Paper Code 2004-01-1379.
[3] Vargas JVC, Parise JAR. Simulation in transient regime of a heat pump with closed-loop and oneoff control. Int J Refrig 1995;18:235–43.
[4] Antonijevic D, Heckt R. Heat pump supplemental heating system for motor vehicles. Proc Inst Mech Eng, D J Automob Eng 2004;218:1111–15.
[5] Domitrovic ER, Mei VC, Chen FC. Simulation of an automotive heat pump. ASHRAE Trans; 1997;1:291–96.
[6] Hosoz M, Direk M. Performance evaluation of an integrated automotive air conditioning and heat pump system. Energy Convers Manag;2006; 47:545–59.
[7] Rongstam J, Mingrino FA. A coolant-based automotive heat pump system. Vehicle Thermal Management Systems Conference Proceedings 2003; SAE Paper Code C599/067/2003.
[8] Lee DY, Cho CW, Won JP, Park YC, Lee MY. Performance characteristics of mobile heat pump for a large passenger electric vehicle. Appl Therm Eng 2013:50;660–69.
[9] Scherer LP, Ghodbane M, Baker JA, Kadle PS. On-vehicle performance comparison of an R-152a and R-134a heat pump system. SAE Technical Papers 2003; Paper code 2003-01-0733.
[10] Direk M, Hosoz M. Energy and exergy analysis of an automobile heat pump system. Int J Exergy 2008;5:556–66.
[11] Tamura T, Yakumaru Y, Nishiwaki F. Experimental study on automotive cooling and heating air conditioning system using CO2 as a refrigerant. Int J Refrig 2005;28:1302–07.
[12] Kim SC, Kim MS, Hwang IC, Lim TW. Heating performance enhancement of a CO2 heat pump system recovering stack exhaust thermal energy in fuel cell vehicles. Int J Refrig 2007;3: 1215–26.
[13] Lemmon EW, Huber ML, McLinden MO. NIST reference fluid thermodynamic and transport properties-REFPROP V8.0. National Standards and Technology 2007.
[14] Moffat RJ. Describing the uncertainties in experimental results. Exp Therm Fluid Sci 1988; 1:3–17.